J Low Temp Phys
DOI 10.1007/s10909-014-1238-x

The Limit of Mechanical Stability in Quantum Crystals: A Diffusion Monte Carlo Study of Solid ^{4}He

Claudio Cazorla · Jordi Boronat

Received: 11 August 2014 / Accepted: 26 September 2014

Abstract We present a first-principles study of the energy and elastic properties of solid helium at pressures below the range in which it is energetically stable. We find that the limit of mechanical stability in hcp ^{4}He is $P_s = -33.8(1)$ bar, which lies significantly below the spinodal pressure found in the liquid phase (i.e., -9.6 bar). Furthermore, we show that the pressure variation of the transverse and longitudinal sound velocities close to P_s does not follow a power law of the form $\propto (P - P_s)^\gamma$, in contrast to what is observed in the fluid.

Keywords Solid helium · Elasticity · Metastable

1 Introduction

In the last two decades, extensive theoretical and experimental works have focused on the study of liquid helium at negative pressures and ultra-low temperatures [1,2]. The equation of state of this material has been measured very accurately within the density range in which it is stable, and extrapolated to the region of negative pressures [3, 4]. On the theoretical side, quantum Monte Carlo methods have allowed for precise and explicit simulation of metastable liquid helium, producing results which are in remarkably good agreement with experiments [5]. A quantity of central interest in all these studies is the spinodal pressure P_s, that is, the pressure at which the bulk

C. Cazorla (✉)
School of Materials Science and Engineering, University of New South Wales, Sydney, NSW 2052, Australia
e-mail: ccazorla@icmab.es

J. Boronat
Departament de Física i Enginyeria Nuclear, Universitat Politècnica de Catalunya, Campus Nord B4-B5, Barcelona 08034, Spain

Published online: 09 October 2014

modulus, B, and sound velocity vanish and thus, the liquid becomes unstable against long wavelength density fluctuations. In liquid ^{4}He, P_s amounts to -9.6 bar, while in liquid ^{3}He to -3.2 bar [3,4].

Analogous studies performed in solid helium are almost non-existent in the literature [6,7]. At $T = 0$ K, solid helium becomes stable at pressures larger than ~ 25 bar; thus certainly, the realm of negative pressures lies well below such a threshold. Nevertheless, analysis of the mechanical stability limit in helium crystals turns out to be a topic of fundamental interest because of the extraordinary degree of quantumness of these systems. In contrast to liquids, solids can sustain shear stresses, and because of this ordinary fact, the definition of the spinodal point in crystals differs greatly from the one given above. In the particular case of solid ^{4}He, previous attempts to determine P_s have been, to the best of our knowledge, only tentative [6,7].

The energy of a crystal under a homogeneous elastic deformation can be expressed as

$$E(V, \eta) = E(V, 0) + \frac{1}{2} V \sum_{ij} C_{ij} \eta_i \eta_j, \tag{1}$$

where $\{C_{ij}\}$ are the elastic constants, $\{\eta_i\}$ a small strain deformation (both expressed in Voigt notation), and $E(V, 0)$ the energy of the undistorted equilibrium system. The specific symmetry of a crystal determines the number of independent elastic constants which are different from zero. In the case of hexagonal crystals (e.g., hcp ^{4}He), these are five: C_{11}, C_{12}, C_{13}, C_{33}, and C_{44}. The conditions for mechanical stability in a crystal follow from the requirement that upon a general strain deformation, the change in the total energy must be positive. It can be shown that in hcp crystals subject to an external pressure P these conditions readily are [8,9]

$$\begin{aligned} &C_{44} - P > 0 \,[\text{C1}] \\ &C_{11} - C_{12} - 2P > 0 \,[\text{C2}] \\ &(C_{33} - P)\,(C_{11} + C_{12}) - 2\,(C_{13} + P)^2 > 0 \,[\text{C3}]. \end{aligned} \tag{2}$$

The spinodal pressure, or limit of mechanical stability, in a crystal then is identified with the point at which any of the three conditions above is violated. We must note that the bulk modulus of an hexagonal crystal can be expressed as [10]

$$B = -V \frac{dP}{dV} = \frac{C_{33}\,(C_{11} + C_{12}) - 2C_{13}^2}{C_{11} + C_{12} + 2C_{33} - 4C_{13}}; \tag{3}$$

thus, the conditions at which the bulk modulus vanishes in general must not coincide with the corresponding limit of mechanical stability. This reasoning is in fact very different from the usual P_s analysis performed in liquids.

In this article, we present a computational study of the energetic and elastic properties in solid ^{4}He at pressures below ~ 25 bar, based on the diffusion Monte Carlo method. Our first-principles calculations allow us to determine with precision the limit of mechanical stability in this crystal, which we estimate to be $P_s = -33.8(1)$ bar

(that is, much larger in absolute value than the one estimated for the fluid). Moreover, we show that, in contrast to liquid helium, the pressure variation of the sound velocities near P_s does not follow a power law of the form $\propto (P - P_s)^{\gamma}$ with $\gamma = 1/3$ [11].

The organization of this article is as follows. In the next section, we provide the details of our computational method and calculations. In Sect. 3, we present our results and comment on them. Finally, we summarize our main findings in Sect. 4.

2 Computational Details

In DMC, the time-dependent Schrödinger equation of a N-particle system is solved stochastically by simulating the time evolution of the Green's function propagator $e^{-\frac{i}{\hbar}\hat{H}t}$ in imaginary time $\tau \equiv \frac{it}{\hbar}$. In the $\tau \to \infty$ limit, sets of configurations (walkers) $\{\mathbf{R}_i \equiv \mathbf{r}_1, \ldots, \mathbf{r}_N\}$ render the probability distribution function $\Psi_0\Psi$, where Ψ_0 is the true ground-state wave function and Ψ a guiding wave function used for importance sampling. Within DMC, virtually exact results (i.e., subject to statistical uncertainties only) can be obtained for the ground-state energy and related quantities [12,13].

We are interested in studying the ground-state of hcp ^{4}He, which we assume to be governed by the Hamiltonian $H = -\frac{\hbar^2}{2m_{\mathrm{He}}}\sum_{i=1}^{N}\nabla_i^2 + \sum_{i<j}^{N} V_{\mathrm{He-He}}(r_{ij})$, where m_{He} is the mass of a ^{4}He atom and $V_{\mathrm{He-He}}$ the semi-empirical pairwise potential due to Aziz [14]. It is worth noticing that the Aziz potential provides an excellent description of the He–He interactions at low pressures [15,20].

The guiding wave function that we use in this study, Ψ_{SNJ}, reproduces both the crystal ordering and Bose–Einstein symmetry. This model wave function was introduced in Ref. [16] and it reads

$$\Psi_{\mathrm{SNJ}}(\mathbf{r}_1, \ldots, \mathbf{r}_N) = \prod_{i<j}^{N} f(r_{ij}) \prod_{J=1}^{N}\left(\sum_{i=1}^{N} g(r_{iJ})\right), \tag{4}$$

where index J in the second product runs over the equilibrium lattice positions. In previous works, we have demonstrated that Ψ_{SNJ} provides an excellent description of the ground-state properties of bulk hcp ^{4}He [16] and quantum solid films [17–19]. Here, we adopt the correlation functions in Eq. (4) of the McMillan, $f(r) = \exp\left[-1/2\,(b/r)^5\right]$, and Gaussian, $g(r) = \exp\left[-1/2\,(ar^2)\right]$, forms, and optimize the corresponding parameters with variational Monte Carlo (VMC) [in order to simulate the metastable solid, we performed one unique VMC optimization at $P \sim 25$ bar].

The technical parameters in our calculations were set in order to ensure convergence of the total energy per particle to less than 0.02 K/atom. The value of the mean population of walkers was 500 and the length of the imaginary time-step ($\Delta\tau$) 5×10^{-4} K^{-1}. We used large simulation boxes containing 200 atoms in all the cases. Statistics were accumulated over 10^5 DMC steps performed after system equilibration, and the approximation used for the short-time Green's function $e^{-\hat{H}\tau}$ is accurate to second order in τ [20,21].

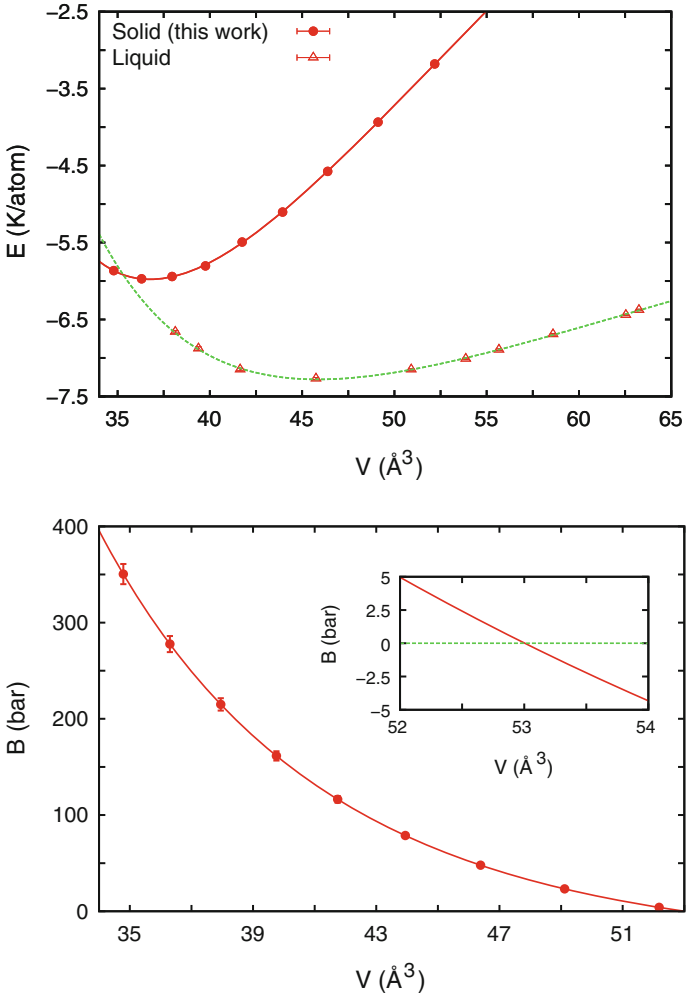

Fig. 1 *Top* Calculated equilibrium energy per particle expressed as a function of volume. The *solid line* represents a polynomial fit to our results (see text). Results obtained in the liquid phase (from work [5]) are shown for comparison. *Bottom* Calculated bulk modulus expressed as a function of volume. The region in which B vanishes is augmentated on the *inset* (Color figure online)

The computational strategy that we followed to calculate the elastic constants $\{C_{ij}\}$ is the same as explained in Refs. [10,22,23]; thus, we address the interested reader to them.

3 Results and Discussion

In Fig. 1, we show the calculated energy in solid helium expressed as a function of volume (solid symbols). We optimized the c/a ratio in all the considered structures and found that, within our statistical uncertainties, this quantity always amounts to 1.63. We fitted our results to the polynomial curve

$$E(V,0) = E_0 + b\left[\left(\frac{V_0}{V}\right) - 1\right]^2 + c\left[\left(\frac{V_0}{V}\right) - 1\right]^3, \quad (5)$$

and found as best parameters $E_0 = -5.978(5)$ K, $V_0 = 36.90(5)$ Å^3, $b = 34.38(5)$ K, and $c = 7.86(5)$ K. In comparison with the analogous energy curve obtained in the liquid (see Fig. 1) [5], $E(V,0)$ displays larger slopes, which translates into larger negative pressures, at volumes close to equilibrium (i.e., V_0). In the same figure, we enclose the bulk modulus, $B(V) = Vd^2E/dV^2$, that is calculated directly from $E(V,0)$ [solid line]. The symbols which appear therein correspond to estimations obtained with Eq. (3), thereby excellent consistency between our energy and C_{ij} calculations is demonstrated. We find that the bulk modulus of helium vanishes at volume $V_B = 53.00(5)$ Å^3 and pressure $P_B = -34.1(1)$ bar. In what follows, we present our analysis of the elastic properties and mechanical stability in solid ^{4}He and clarify whether V_B and P_B are meaningful physical quantities.

Figure 2 shows how the calculated elastic constants in solid helium change as a function of volume. As expected, all five C_{ij} decrease with increasing volume. In particular, C_{12} and C_{13} become zero at $V = 48.32(5)$ [$P = -32.8(1)$ bar] and $44.95(5)$ Å^3 [$-29.5(1)$ bar]. We performed power-law fits to our $C_{ij}(V)$ results in order to render continuous elastic constant functions. By doing this, we were able to represent the three conditions of mechanical stability in hcp helium [see Eq. (2)] within the volume interval of interest. These results are enclosed in Fig. 3, where it is shown that condition 3, i.e., [C3] in Eq. (2), is violated at $V_s = 50.81(5)$ Å^3 and $P_s = -33.8(1)$ bar. Thus, we identify (V_s, P_s) with the limiting state at which solid ^{4}He remains mechanically stable. We note that these conditions, although not identical, are very similar to (V_B, P_B), namely the state at which the bulk modulus vanishes [as it now follows from Eqs. (2), (3)].

Interestingly, the mechanical stability limit that we predict for hcp ^{4}He is well below the spinodal pressure found in liquid helium (i.e., $P_s^{\text{liquid}} = -9.6$ bar). In order to understand the physical origins behind such a large difference, we analyzed the volume expansion that both liquid and solid systems undergo from equilibrium to their corresponding spinodal limits, namely $\Delta V/V_0 \equiv (V_s - V_0)/V_0$. We find that $\Delta V/V_0$ actually amounts to $\sim 38\ \%$ in both liquid and solid phases (i.e., $V_0^{\text{solid}} = 36.90(5)$, $V_s^{\text{solid}} = 50.81(5)$, and $V_0^{\text{liquid}} = 45.75(5)$, $V_s^{\text{liquid}} = 63.25(5)$ Å^3, where the data for the liquid phase have been extracted from Ref. [5]). This last outcome and the two equations of state shown in Fig. 1 appear to clarify the root of the large $|P_s^{\text{solid}} - P_s^{\text{liquid}}|$ difference: before becoming mechanically unstable helium endures a relative volume expansion that is more or less independent on the structure; the accompanying energy increase in the crystal, however, is much larger than that in the liquid, essentially because of the constrained motion of the atoms in the former, and thus $|P_s^{\text{solid}}| \gg |P_s^{\text{liquid}}|$ follows.

Sound velocities in solids can be either longitudinal or transverse and depend on the direction of propagation. In crystals with hexagonal symmetry, two main propagation modes are identified, one along the c-axis and the other contained in the basal plane. The relationships between the elastic constants and sound velocities in hcp crystals are

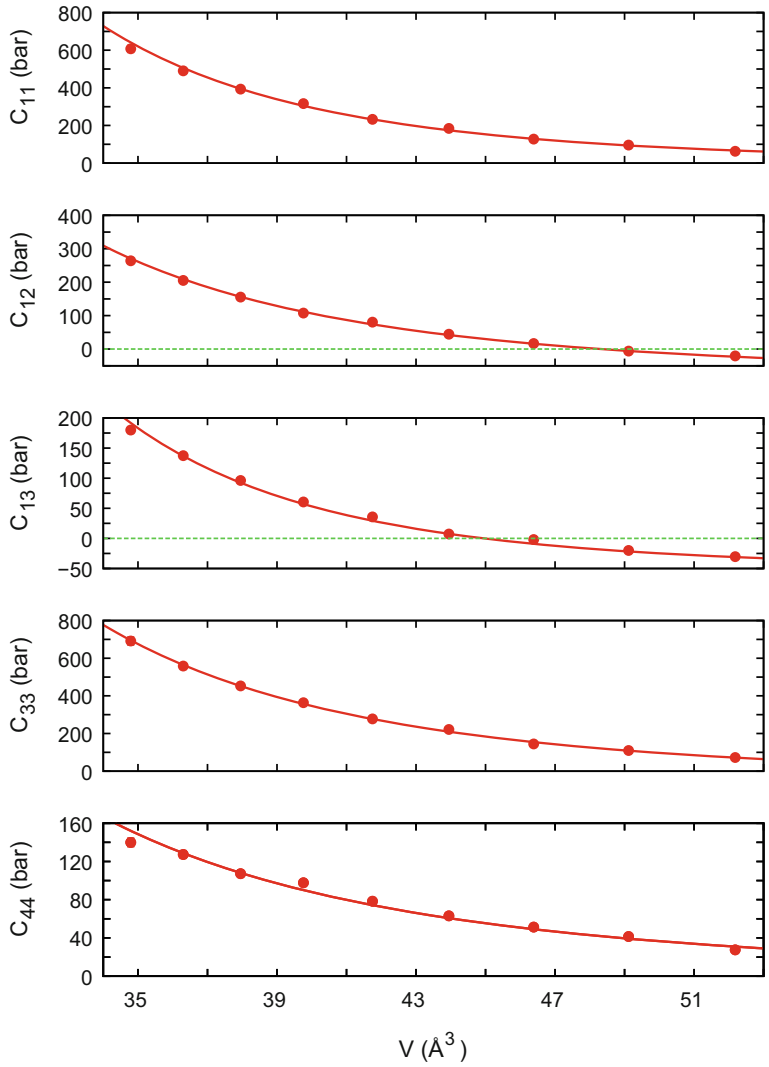

Fig. 2 Calculated elastic constants expressed as a function of volume. The *solid lines* are power-law fits to our results (*solid symbols*) (Color figure online)

$$\begin{aligned} v_L &= (C_{33}/\rho)^{1/2} \\ v_{T1} &= v_{T2} = (C_{44}/\rho)^{1/2} \end{aligned} \tag{6}$$

along the c-axis, and

$$\begin{aligned} v_L &= (C_{11}/\rho)^{1/2} \\ v_{T1} &= \left(\frac{C_{11} - C_{12}}{2\rho}\right)^{1/2} \\ v_{T2} &= (C_{44}/\rho)^{1/2} \end{aligned} \tag{7}$$

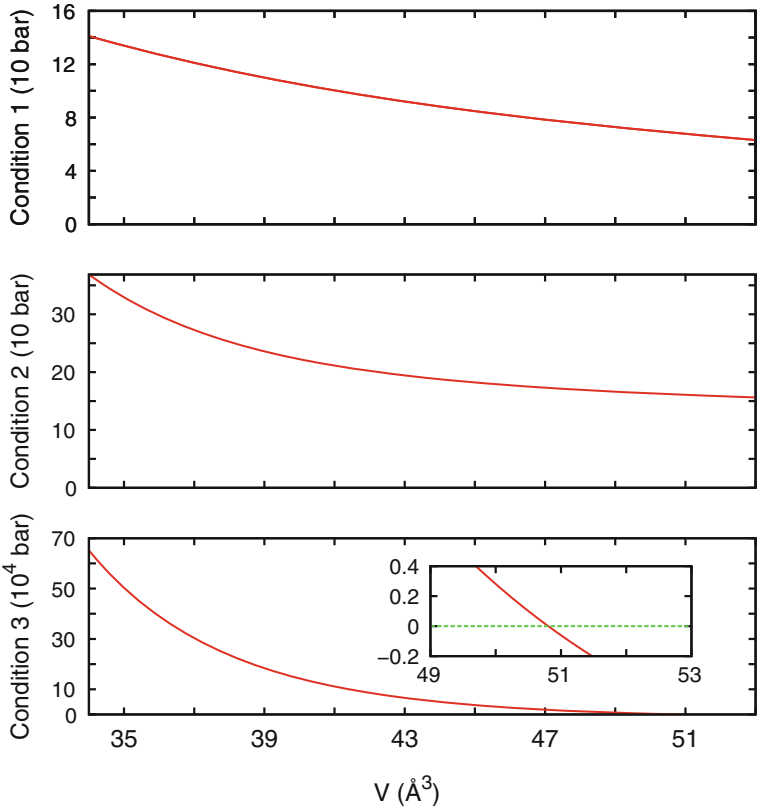

Fig. 3 Conditions of mechanical stability [see Eq. (2)] expressed as a function of volume. The region in which condition 3 is not accomplished is augmentated on the *inset* (Color figure online)

in the basal plane [10]. In Fig. 4, we plot the six c-axis and basal sound velocities calculated in solid helium as a function of pressure (some of them are coincident) together with an appropriate average, v_D [10]. We observe that none of the sound velocities vanishes at the spinodal pressure P_s (marked in red in the figure), as it was already expected from Eqs. (2), (6), (7). Moreover, in Fig. 5, we plot the angular dependence of the (now pseudo) longitudinal and transverse sound velocities [24,25] calculated in the mechanical stability limit; there, ϕ represents the angle between the sound wave direction and the c-axis in the crystal (i.e., $\phi = 0°, 90°$ corresponds to the c-axis and basal plane cases, respectively). It is observed that despite v_L reaches a minimum at $\phi = 48.3°$, none of the three sound velocities vanishes at P_s. We also find that all sound velocities are larger than zero at P_B, the pressure at which the bulk modulus vanishes, independently of ϕ (not shown in the figure). From the present analysis, it is deduced that any of the normal modes that should vanish at P_s is non-acoustic. Unfortunately, we are not able to identify those modes with the present approach.

Recently, it has been suggested that the variation of the sound velocities near the spinodal density in hcp ^{4}He could follow a power law of the form $\propto (P - P_s)^\gamma$, where

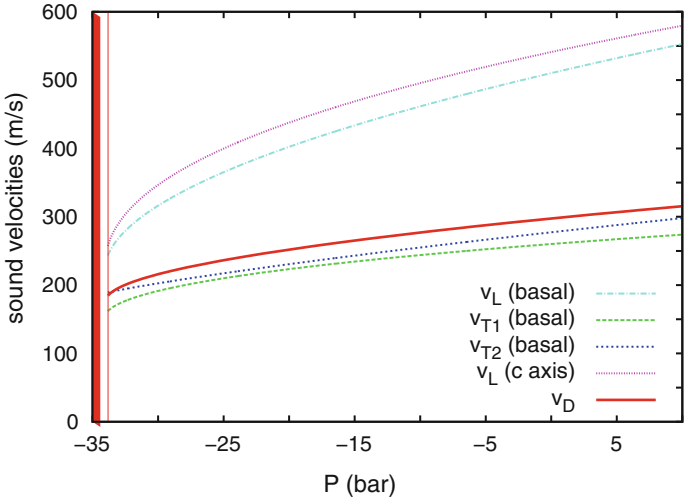

Fig. 4 Calculated sound velocities along the c-axis and in the basal plane [see Eqs. (6), (7)] expressed as a function of pressure. The region in which the crystal becomes mechanically unstable is filled with *red color* (Color figure online)

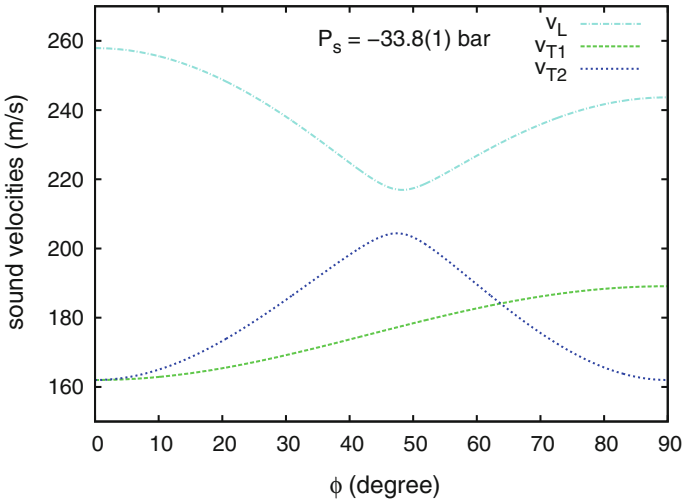

Fig. 5 Angular dependence of the calculated sound velocities in hcp ^{4}He at the limit of mechanical stability (see Refs. [24,25]) (Color figure online)

$\gamma = 1/3$, in analogy to what is observed in the liquid phase [6,7]. However, in light of the results presented in Figs. 4 and 5, such hypotheses must be rejected because none of the sound velocities becomes zero at P_s. Furthermore, we performed analytical fits of the form $v_{L,T}(P) = a + b\,(P - P_s)^{\beta}$ to our results and found that parameter β was always different from $1/3$. For instance, in the v_D case, we found $\beta = 0.55(2)$ as the optimal value. Therefore, we must conclude that propagation of sound waves in helium crystals at the verge of mechanical instability differs radically from that in liquid helium under similar conditions.

4 Conclusions

We have presented a rigorous and precise computational study of the energy and elastic properties of solid helium at conditions in which it is metastable. We have determined the limit of mechanical stability in this crystal, i.e., $P_s = -33.8(1)$ bar, and the variation of the sound velocities at pressures close to it. Overall, we demonstrated that solid and liquid helium behave radically different in the vicinity of their spinodal limits.

Acknowledgments This work was supported by MICINN-Spain [Grants Nos. MAT2010-18113, CSD 2007-00041, FIS2011-25275, and CSIC JAE-DOC program (C.C.)], and Generalitat de Catalunya [Grant No. 2009SGR-1003].

References

1. J.A. Nissen, E. Bodegom, L.C. Brodie, J.S. Semura, Phys. Rev. B **40**, 6617 (1989)
2. H.J. Maris, S. Balibar, M.S. Pettersen, J. Low Temp. Phys. **93**, 1069 (1993)
3. H.J. Maris, J. Low Temp. Phys. **98**, 403 (1995)
4. H.J. Maris, D.O. Edwards, J. Low Temp. Phys. **129**, 1 (2002)
5. J. Boronat, J. Casulleras, J. Navarro, Phys. Rev. B **50**, 3427 (1994)
6. H.J. Maris, J. Low Temp. Phys. **155**, 290 (2009)
7. H.J. Maris, J. Low Temp. Phys. **158**, 485 (2010)
8. G.V. Sin'ko, N.A. Smirnov, J. Phys. Condens. Matter **14**, 6989 (2002)
9. G. Grimvall et al., Rev. Mod. Phys. **84**, 945 (2012)
10. C. Cazorla, Y. Lutsyshyn, J. Boronat, Phys. Rev. B **85**, 024101 (2012)
11. H.J. Maris, Phys. Rev. Lett. **66**, 45 (1991)
12. R. Barnett, P. Reynolds, W.A. Lester Jr, J. Comput. Phys. **96**, 258 (1991)
13. J. Casulleras, J. Boronat, Phys. Rev. B **52**, 3654 (1995)
14. R.A. Aziz, F.R.W. McCourt, C.C.K. Wong, Mol. Phys. **61**, 1487 (1987)
15. C. Cazorla, J. Boronat, J. Phys. Condens. Matter **20**, 015223 (2008)
16. C. Cazorla, G. Astrakharchick, J. Casulleras, J. Boronat, N. J. Phys. **11**, 013047 (2009)
17. C. Cazorla, J. Boronat, Phys. Rev. B **77**, 024310 (2008)
18. C. Cazorla, G. Astrakharchick, J. Casulleras, J. Boronat, J. Phys. Condens. Matter **22**, 165402 (2010)
19. M.C. Gordillo, C. Cazorla, J. Boronat, Phys. Rev. B **83**, 121406(R) (2011)
20. J. Boronat, J. Casulleras, Phys. Rev. B **49**, 8920 (1994)
21. S.A. Chin, Phys. Rev. A **42**, 6991 (1990)
22. C. Cazorla, Y. Lutsyshyn, J. Boronat, Phys. Rev. B **87**, 214522 (2013)
23. R. Rota, Y. Lutsyshyn, C. Cazorla, J. Boronat, J. Low Temp. Phys. **168**, 150 (2012)
24. C.-S. Zha, T.S. Duffy, H.-K. Mao, R.J. Hemley, Phys. Rev. B **48**, 9246 (1993)
25. M.J.P. Musgrave, *Crystal Acoustics* (Holden-Day, San Francisco, 1970)